VIP Sodium Full Cells Very Important Paper

International Edition: DOI: 10.1002/anie.201505215
German Edition: DOI: 10.1002/ange.201505215

A High-Voltage and Ultralong-Life Sodium Full Cell for Stationary Energy Storage

*Shaohua Guo, Pan Liu, Yang Sun, Kai Zhu, Jin Yi, Mingwei Chen, Masayoshi Ishida, and Haoshen Zhou**

Abstract: *Recently, there has been great interest in developing advanced sodium-ion batteries for large-scale application. Most efforts have concentrated on the search for high-performance electrode materials only in sodium half-cells. Research on sodium full cells for practical application has encountered many problems, such as insufficient cycles with rapid capacity decay, low safety, and low operating voltage. Herein, we present a layered P2-$Na_{0.66}Ni_{0.17}Co_{0.17}Ti_{0.66}O_2$, as both an anode (ca. 0.69 V versus Na^+/Na) and as a high-voltage cathode (ca. 3.74 V versus Na^+/Na). The full cell based on this bipolar electrode exhibits well-defined voltage plateaus near 3.10 V, which is the highest average voltage in the symmetric cells. It also shows the longest cycle life (75.9% capacity retention after 1000 cycles) in all sodium full cells, a usable capacity of 92 mAh g^{-1}, and superior rate capability (65 mAh g^{-1} at a high rate of 2C).*

An inexpensive and efficient energy storage device is urgently required for the smooth integration of renewable energy into a smart grid on a large scale.[1] The increasing cost and limited availability of lithium suggest that an alternative to lithium-ion batteries should be developed to meet this need.[2] Sodium-ion batteries (SIBs) have a similar chemical storage mechanism as their lithium-ion counterparts, and are expected to be low cost and chemically sustainable owing to an almost infinite supply of sodium.

The important properties of stationary batteries for electrical energy storage (EES) are long life, high safety, high efficiency, and low cost. These are more essential factors than capacity, and definitely different from the requirements for power batteries.[3] However, recent research efforts have encountered numerous problems, such as low safety resulting from the low anode plateau near the sodium plating voltage and limited cycle life with rapid capacity decay. On the anode side, hard carbon has mostly been demonstrated to show a large capacity,[4] but most discharge capacity is distributed in the potential region 0–0.1 V versus Na^+/Na, thereby leading to potential safety concerns. Several oxides such as $Na_2Ti_3O_7$[5] and alloy compounds[6] (P, Sn, or Sb) always undergo large volume changes (420% for Sn) during the insertion and extraction of Na ions, and would not be suitable for long-life batteries. On the cathode side, the large Na ions with an ionic radius of 1.02 Å readily induce the phase transition, especially for layered sodium oxides such as O3-P3[7] and P2-O2.[8] This phase transformation causes a serious decrease in the capacity and a short cycle life.[9] Therefore, sodium full cells with a sodium storage cathode and nonmetallic sodium anode are far from a satisfactory breakthrough, and the development of highly safe and long-lifetime sodium full cells is still a great challenge.

Herein, we firstly report a bipolar electrode material with a high cycling stability, P2-$Na_{0.66}Ni_{0.17}Co_{0.17}Ti_{0.66}O_2$, which not only exhibits a remarkable high average voltage of about 3.74 V versus Na^+/Na in the cathode side, but also delivers a very safe potential of approximately 0.69 V at the anode side. Electrochemical results clearly reveal that this material shows superior cycling stability in both the cathode and anode sides. The symmetric sodium full cells based on this bipolar material show an ultralong cycle life (94.8% capacity retention after 100 cycles, 75.9% capacity retention after 1000 cycles), a high operating voltage of about 3.10 V, and superior rate capability (65 mAh g^{-1} capacity at a high rate of 2C). It will greatly contribute to the development of sodium full cells towards stationary applications, and also provide new avenues for designing advanced electrode materials for sodium-ion batteries.

Figure 1a shows a schematic representation of symmetric sodium-ion batteries. In this study, P2-$Na_{0.66}Ni_{0.17}Co_{0.17}Ti_{0.66}O_2$ was developed as a bipolar electrode material that simultaneously serves as the cathode and anode. In addition to the same Al current collectors (no alloying reaction between Na and Al) for both the positive and negative electrodes, the substantial cost will be greatly reduced in the production process. A safe voltage plateau of approximately 0.7 V has been validated in layered titanium-based oxides,[10] and will ensure the safety of full cells. Noticeably, a voltage of about 3.74 V when using this material as cathode will greatly promote the output voltage and energy density in full cells. Figure 1b illustrates that our novel symmetric cells can

[*] S. H. Guo, Dr. Y. Sun, K. Zhu, Dr. J. Yi, Prof. H. S. Zhou
Energy Technology Research Institute, National Institute of Advanced Industrial Science and Technology (AIST)
Umezono 1-1-1, Tsukuba 305-8568 (Japan)
E-mail: hs.zhou@aist.go.jp
S. H. Guo, Prof. M. Ishida, Prof. H. S. Zhou
Graduate School of System and Information Engineering
University of Tsukuba, Tennoudai 1-1-1, Tsukuba 305-8573 (Japan)
Dr. P. Liu, Prof. M. W. Chen
WPI Advanced Institute for Materials Research
Tohoku University, Sendai 980-8577 (Japan)
Prof. H. S. Zhou
National Laboratory of Solid State Microstructures &
Department of Energy Science and Engineering
Nanjing University, Nanjing 210093 (China)
E-mail: hszhou@njedu.cn

Supporting information for this article is available on the WWW under http://dx.doi.org/10.1002/anie.201505215.

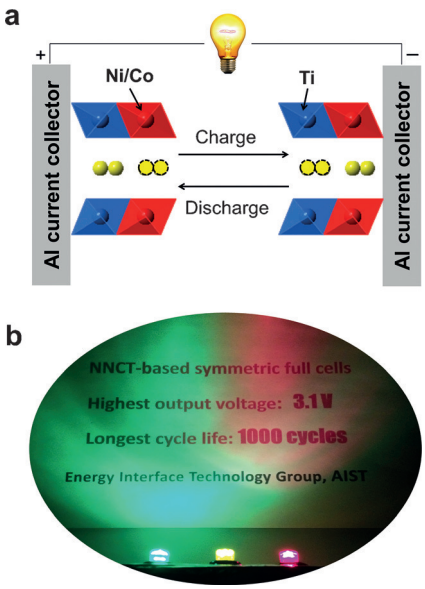

Figure 1. a) A diagram of the proposed symmetric cell based on P2-$Na_{0.66}Ni_{0.17}Co_{0.17}Ti_{0.66}O_2$. The different redox centers (Ni/Co for cathode and Ti for anode) exist in the layered structure, where the black dotted circles represent the corresponding active sodium ions. b) Optical image showing the lit LED bulbs driven by the designed bipolar $Na_{0.66}Ni_{0.17}Co_{0.17}Ti_{0.66}O_2$-based symmetric cells.

successfully light LED lamps after charging to 3.5 V versus Na^+/Na.

Figure 2a shows Rietveld plots of P2-$Na_{0.66}Ni_{0.17}Co_{0.17}Ti_{0.66}O_2$ (hereafter denoted as P2-NNCT), and all the diffraction lines can be indexed to a hexagonal lattice with space group *P*63/mmc. The lattice parameters are refined to $a = b = 2.9537(1)$, $c = 11.1503(2)$ Å, and $V = 84.250(5)$ Å^3 with convergence R_{wp} factors (5.54%) and a χ^2 (2.721) value using the GSAS + EXPGUI suite[11] (detailed crystallographic data on refined P2-$Na_{0.66}Ni_{0.17}Co_{0.17}Ti_{0.66}O_2$ are listed in Table S1). The scanning electron microscopy (SEM) image in Figure 2b shows that the particle size of the P2-NNCT samples ranges from 2 to 5 μm. Detailed structural information on P2-NNCT samples was obtained by scanning area electron diffraction (SAED) and scanning transmission electron microscopy studies (STEM; Figure 2c–h; the representative particle that we chose for study is shown in Figure S1). The bright spots viewed along the 010 and 001 directions in Figure 2c,d, respectively, are indexed to the typical reflections originating from the P2 layered structure. The local structure of P2-NNCT materials were analyzed with atomic resolution by high-angle annular dark field (HAADF) and annular bright field (ABF) STEM. The bright-dot contrast in the HAADF-STEM images (Figure 2e) and the dark-dot contrast in the ABF-STEM images (Figure 2f) reveal the column positions of the transition-metal atoms (Ni, Co, and Ti). The faint dark-dot contrast with the interlayer positions in the ABF-STEM images (Figure 2f) corresponds to the column positions of the sodium and oxygen atom in these two layered structures. As shown in Figure 2g,h, the high-resolution STEM images (enlarged from Figure 2e,f, respectively) reveal the detailed atomic arrangements with regard to P2 ABBA stacking, and the atomic models of layered P2 structures are inserted for convenient visualization. The ABF-STEM observations of octahedral TMO_2 (TM = Ni, Co, and Ti) are highly consistent with the structural model. The sodium atoms are clamped by layered TMO_2. In particular, every two layers of TMO_2 are structurally mirror-symmetric for the P2 phase. Electron energy loss spectroscopy (EELS) mapping was carried out (in the white rectangle frame shown in Figure S2, and clearly shows that the sodium, cobalt, nickel, titanium, and oxygen elements are uniformly distributed in the particle.

The electrochemical properties of P2-NNCT as a bipolar material were assessed by a constant charge/discharge test in the half cells versus Na^+/Na. Figure 3a shows the typical charge/discharge cycle at the cathode side from 2 to 4 V at a rate of 0.2C. A reversible capacity of 55 mAh g^{-1} can be

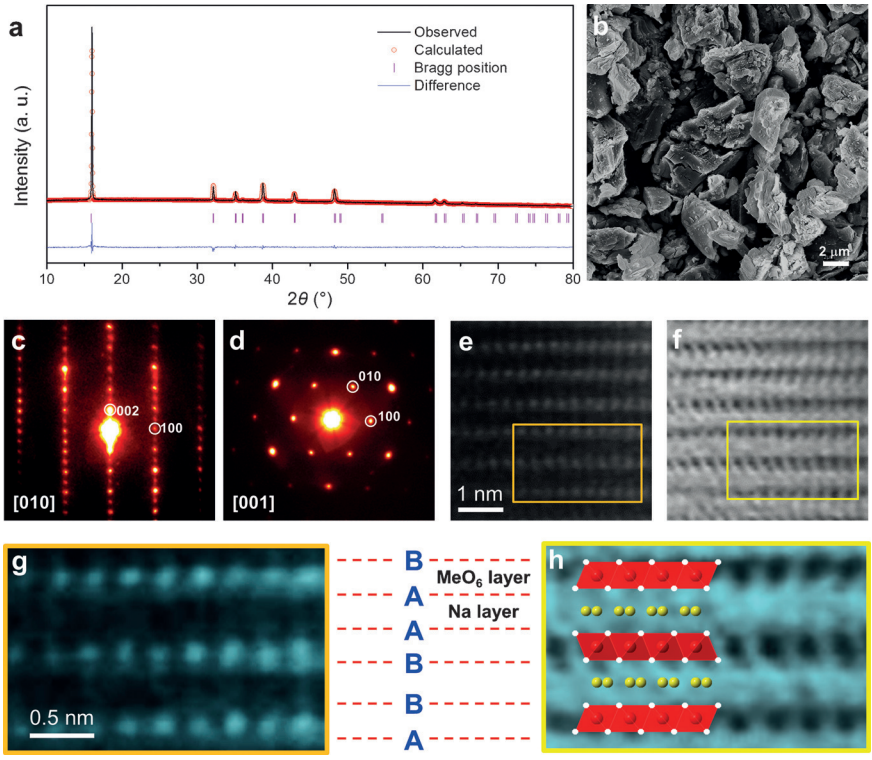

Figure 2. a) XRD and Rietveld plots of P2-NNCT compounds with experimental data in black dots, calculated curves in red, and difference curve in blue, as well as standard Bragg reflections as pink vertical bars. b) SEM images of P2-NNCT samples. c,d) SAED patterns of P2-NNCT viewed along the [010] and [001] zone axis, respectively. e) HADDF-STEM image of P2-NNCT. f) ABF-STEM image of P2-NNCT. g,h) enlarged STEM images extracted from (e) and (f), showing the ABBAAB (from bottom to top) stacking of P2 structures.

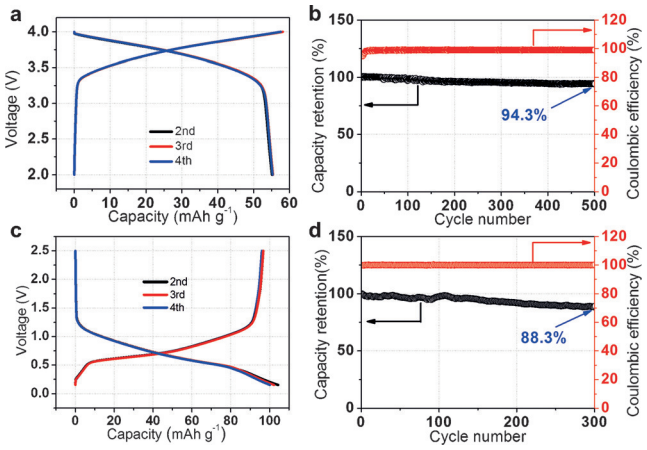

Figure 3. The electrochemical performance of P2-NNCT compounds in half cells. a) The typical charge/discharge profiles between 2 and 4 V at a rate of 0.2C. b) The corresponding cycling performance with coulombic efficiency over 500 cycles at a rate of 0.2C. c) The typical discharge/charge profiles between 0.15 and 2.5 V at a rate of 0.2C. d) The corresponding cycling performance with coulombic efficiency over 300 cycles at a rate of 0.2C.

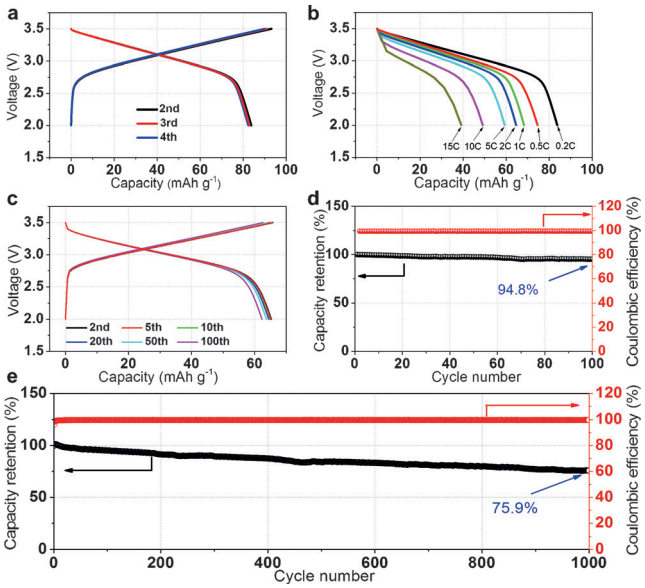

Figure 4. The electrochemical performance of bipolar NNCT-based symmetric full cells. a) The typical charge/discharge profiles between 2 and 3.5 V at a rate of 0.2C (a rate of 1C corresponds to 100 mA g^{-1}). b) The capacity at different rates of 0.2C, 0.5C, 1C, 2C, 5C, 10C, and 15C. c) The charge/discharge profiles of the 2nd, 5th, 10th, 20th, 50th, and 100th cycles with a rate of 1C showing no apparent decay in the voltage and capcity. d) The capacity retention with coulombic efficiency at a rate of 1C. e) The capacity retention with coulombic efficiency at a rate of 5C, showing the outstanding cycling performance (75.9% capacity retention after 1000 cycles).

obtained in the first and following cycles, and shows a very high average voltage of about 3.74 V, smooth charge/discharge profiles, and little polarization. The highly overlapped dQ/dV curves (see Figure S4a) suggest a good reversibility of this cathode. The cycling stability and corresponding coulombic efficiency of P2-NNCT as a cathode was also evaluated (Figure 3b). The capacity after 500 cycles is very close to the initial capacity, even with the deep charging and discharging at a rate of 0.2C, and the corresponding retention is 94.3%. The rate of capacity decay is only about 0.011% per cycle, which is indicative of a high cycling stability, and is the best cyclability of all the reported positive electrode materials to our knowledge. All the Coulombic efficiencies (except for initial cycles) of this electrode material are about 99.9%. The typical discharge/charge voltage profiles of P2-NNCT as a negative electrode are displayed in Figure 3c. It shows a large reversible discharge capacity of 105 mAh g^{-1} along with a clear step around 0.69 V in the initial and subsequent cycles. The coincident dQ/dV curves (Figure S4b) indicate the good reversibility of this electrode. The cycle stability and corresponding coulombic efficiency were also measured (Figure 3d). The capacity retention after 300 cycles is maintained at 88.3%, and the coulombic efficiency except for initial cycles can reach nearly 100% in the whole cycling processes. This most appealing sodium storage performance combined with the excellent long-time cycle stability and Coulombic efficiency of the P2-NNCT in half cells is beneficial to the enhancement of electrochemical performance when assembled in full cells.

NNCT-based full cells were assessed using a constant charge/discharge test in the different voltage ranges of 0.6–3.8 V (Figure S5) and 2–3.5 V (Figure 4). It can deliver a large capacity of 92 mAh g^{-1} between 0.6 and 3.8 V, and the energy density of this full cell is calculated to be about 95 Wh kg^{-1} on the basis of the total cathode and anode mass. Figure 4a illustrates the typical charge/discharge profiles of the full cell with the optimized voltage range of 2.0–3.5 V. A reversible capacity of 84 mAh g^{-1} was obtained in the first cycle (Figure S3c) and subsequent cycles (Figure 4a) at a rate of 0.2C. Surprisingly, this full coin cell could produce an output with a high average potential of approximately 3.10 V, which is comparable to the commercial lithium-ion batteries such as $LiFePO_4$ || graphite. The elevated voltage could be ascribed to the Co substitution in the layered P2 structure.[12] The cathode potential plateau of P2-NNCT is more evident, and in particular is higher than that of $Na_{0.8}Ni_{0.4}Ti_{0.6}O_2$ (Figure S6a), thereby resulting in a remarkable increase in the potential in full cells (Figure S6b). The full cells were also tested at different rates of 0.2C, 0.5C, 1C, 2C, 5C, 10C, and 15C (Figure 4b). The capacity varies from 65 mAh g^{-1} at a 2C rate to 59 mAh g^{-1} at a 5C rate. Even with a discharge rate of 10C, the discharge capacity remains at 50 mAh g^{-1}, approximately 60% of the reversible capacity at a rate of 0.2C. The cycling performance and the corresponding coulombic efficiency were first tested at a rate of 1C (Figure 4d, the corresponding charge/discharge profile at different cycles are displayed in Figure 4c), and there is no apparent degradation in the voltage and capacity over 100 cycles. Note that the defined voltage plateau and the absence of a voltage drop with an increase in cycling are very important for practical application. The full cell offers 94.8% capacity retention after 100 desodiation and sodiation processes, and the compelling high voltage and high safety, the outstanding cycle life, and well-defined voltage plateau promise P2-NNCT to be a superior bipolar electrode for stationary batteries. To further study the

long-term cycling performance, the sodium full cell was evaluated over 1000 cycles at a rate of 5C (Figure 4e). In the fast charging and discharging process, a good capacity retention of 75.9% was measured even after 1000 cycles of sodium ion extraction and insertion. A capacity decay of only about 0.024% per cycle was calculated. To date, this is the best cyclability of a reported sodium full cell. Such an exceptional performance of a full cell is mainly attributed to the high-performance bipolar electrode of NNCT, which supplies a highly stable and open layered framework for facile transportation and storage of Na ions. The introduction of Co into the Ni/Ti metal layer is also highly beneficial to the reversibility and kinetics of the extraction and insertion of Na ions. For this NNCT-based full cell, the coulombic efficiency of the whole cycling process is close to 99.9%, except for the initial cycles, and is thus suitable to serve as an energy storage device in practical applications. Recently, many full-cell configurations have been reported, where very huge irreversible loss in capacity was noted with a very poor cycle life of no more than 200 cycles (Table 1). Our optimized sodium symmetric cells based on P2-NNCT outperform all other sodium full cells (Table 1).

Table 1: The sodium storage properties for reported sodium full cells.

Anode||cathode	Cycle life (cycles)	Voltage [V]	Safety[a]	Rate	(A) Symmetric
hard carbon||$NaNi_{0.5}Mn_{0.5}O_2$[4]	20	ca. 3.0	poor	–	asymmetric
hard carbon||$Na_{2-\delta}MHCF$[13]	25	ca. 3.3	poor	–	asymmetric
hard carbon||R-FeHCF[14]	50	ca. 3.0	poor	10C	asymmetric
hard carbon||$Na_{7/9}Cu_{2/9}Fe_{1/9}Mn_{2/3}O_2$[15]	50	ca. 3.5	poor	–	asymmetric
Fe_3O_4|C||$NaNi_{0.25}Fe_{0.5}Mn_{0.25}O_2$[16]	150	ca. 2.4	moderate	10C	asymmetric
SnS_2-rGO||$Na_{0.78}Li_{0.18}Ni_{0.25}Mn_{0.583}O_w$[17]	50	ca. 2.5	moderate	–	asymmetric
$FeSe_2$||$Na_3V_2(PO_4)_3$[18]	200	ca. 1.7	moderate	–	asymmetric
$Na_3Ti_2(PO_4)_3$[19][b]	–	ca. 1.7	good	–	symmetric
$Na_3V_2(PO_4)_3$[20][b]	200	ca. 1.8	good	5C	symmetric
$Na_{0.8}Ni_{0.4}Ti_{0.6}O_2$[10a][b]	150	ca. 2.8	good	1C	symmetric
$Na_{0.6}Cr_{0.6}Ti_{0.4}O_2$[10b][b]	100	ca. 2.5	good	12C	symmetric
$Na_{0.66}Ni_{0.17}Co_{0.17}Ti_{0.66}O_2$ (this work)[b]	1000	ca. 3.1	good	15C	symmetric

[a] The safety issue is basically evaluated by the sodium insertion voltage at the anode side. Otherwise, the conversion mechanism is considered to be moderate in safety, especially during high-rate charge/discharge, and readily leads to the deposition of metallic sodium on the anode. [b] The positive and negative electrode is the same in these symmetric sodium cells, which is considered to greatly reduce the production cost.

In summary, a layered ternary material $Na_{0.66}Ni_{0.17}Co_{0.17}Ti_{0.66}O_2$ with a P2 layered structure was synthesized by a simple solid-state reaction. The crystal structure was characterized at the atomic scale by advanced spherical aberration-corrected electron microscopy. Using this low-cost bipolar electrode, a sodium full cell was tailored to meet the demand of stationary energy storage. This full cell shows the highest operating voltage of 3.1 V of all reported symmetric cells and the longest lifetime of 1000 cycles in all the studies on sodium full cells, as well as performing with a usable capacity of 92 $mAh\,g^{-1}$ and superior rate capability (about 65 $mAh\,g^{-1}$ at a high rate of 2C). These results on a long lifecycle, highly safe, low cost, high efficiency, and high voltage sodium full cell will greatly contribute to the stationary energy storage technology, and will provide new avenues for designing advanced room-temperature sodium-ion batteries. Further work on the electrochemical mechanism, including the influence of Co substitution on the voltage elevation and structural evolution, is currently under investigation.

Acknowledgements

S.H.G. is grateful for financial support from a CSC (China Scholarship Council) scholarship. P.L. and M.C. are sponsored by JST-CREST "Phase Interface Science for Highly Efficient Energy Utilization", JST (Japan).

Keywords: batteries · electrochemistry · sodium · stationary energy storage · ultralong cycle life

How to cite: *Angew. Chem. Int. Ed.* **2015**, *54*, 11701–11705
Angew. Chem. **2015**, *127*, 11867–11871

[1] Z. Yang, J. Zhang, M. C. Kintner-Meyer, X. Lu, D. Choi, J. P. Lemmon, J. Liu, *Chem. Rev.* **2011**, *111*, 3577–3613.
[2] a) D. Kundu, E. Talaie, V. Duffort, L. F. Nazar, *Angew. Chem. Int. Ed.* **2015**, *54*, 3431–3448; *Angew. Chem.* **2015**, *127*, 3495–3513; b) S. W. Kim, D. H. Seo, X. Ma, G. Ceder, K. Kang, *Adv. Energy Mater.* **2012**, *2*, 710–721; c) H. Pan, Y.-S. Hu, L. Chen, *Energy Environ. Sci.* **2013**, *6*, 2338–2360.
[3] J. Liu, J. G. Zhang, Z. Yang, J. P. Lemmon, C. Imhoff, G. L. Graff, L. Li, J. Hu, C. Wang, J. Xiao, *Adv. Funct. Mater.* **2013**, *23*, 929–946.
[4] S. Komaba, W. Murata, T. Ishikawa, N. Yabuuchi, T. Ozeki, T. Nakayama, A. Ogata, K. Gotoh, K. Fujiwara, *Adv. Funct. Mater.* **2011**, *21*, 3859–3867.
[5] P. Senguttuvan, G. L. Rousse, V. Seznec, J.-M. Tarascon, M. R. Palacin, *Chem. Mater.* **2011**, *23*, 4109–4111.
[6] a) Y. Xu, Y. Zhu, Y. Liu, C. Wang, *Adv. Energy Mater.* **2013**, *3*, 128–133; b) Y. Zhu, X. Han, Y. Xu, Y. Liu, S. Zheng, K. Xu, L. Hu, C. Wang, *ACS nano* **2013**, *7*, 6378–6386; c) J. Qian, X. Wu, Y. Cao, X. Ai, H. Yang, *Angew. Chem. Int. Ed.* **2013**, *52*, 4633–4636; *Angew. Chem.* **2013**, *125*, 4731–4734.
[7] a) S. Komaba, N. Yabuuchi, T. Nakayama, A. Ogata, T. Ishikawa, I. Nakai, *Inorg. Chem.* **2012**, *51*, 6211–6220; b) S. Guo, P. Liu, H. Yu, Y. Zhu, M. Chen, M. Ishida, H. Zhou, *Angew. Chem. Int. Ed.* **2015**, *54*, 5894–5899; *Angew. Chem.* **2015**, *127*, 5992–5997.
[8] Z. Lu, J. Dahn, *J. Electrochem. Soc.* **2001**, *148*, A1225–A1229.
[9] N. Yabuuchi, M. Kajiyama, J. Iwatate, H. Nishikawa, S. Hitomi, R. Okuyama, R. Usui, Y. Yamada, S. Komaba, *Nat. Mater.* **2012**, *11*, 512–517.
[10] a) S. Guo, H. Yu, P. Liu, Y. Ren, T. Zhang, M. Chen, M. Ishida, H. Zhou, *Energy Environ. Sci.* **2015**, *8*, 1237–1244; b) Y. Wang, X. Yu, S. Xu, J. Bai, R. Xiao, Y.-S. Hu, H. Li, X.-Q. Yang, L. Chen, X. Huang, *Nat. Commun.* **2013**, 4.

[11] a) A. C. Larson, R. B. Von Dreele, General Structure Analysis System. LANSCE, MS-H805, Los Alamos, New Mexico **1994**; b) B. H. Toby, *J. Appl. Crystallogr.* **2001**, *34*, 210 – 213.
[12] Y. Koyama, I. Tanaka, H. Adachi, Y. Makimura, T. Ohzuku, *J. Power Sources* **2003**, *119*, 644 – 648.
[13] J. Song, L. Wang, Y. Lu, J. Liu, B. Guo, P. Xiao, J.-J. Lee, X.-Q. Yang, G. Henkelman, J. B. Goodenough, *J. Am. Chem. Soc.* **2015**, *137*, 2658 – 2664.
[14] L. Wang, J. Song, R. Qiao, L. A. Wray, M. A. Hossain, Y.-D. Chuang, W. Yang, Y. Lu, D. Evans, J.-J. Lee, *J. Am. Chem. Soc.* **2015**, *137*, 2658 – 2664.
[15] Y. Li, Z. Yang, S. Xu, L. Mu, L. Gu, Y. S. Hu, H. Li, L. Chen, *Adv. Sci.* **2015**, *2*, 1500031.
[16] S.-M. Oh, S.-T. Myung, C. S. Yoon, J. Lu, J. Hassoun, B. Scrosati, K. Amine, Y.-K. Sun, *Nano Lett.* **2014**, *14*, 1620 – 1626.
[17] H. Liu, J. Xu, C. Ma, Y. S. Meng, *Chem. Commun.* **2015**, *51*, 4693 – 4696.
[18] K. Zhang, Z. Hu, X. Liu, Z. Tao, J. Chen, *Adv. Mater.* **2015**, *27*, 3305 – 3309.
[19] P. Senguttuvan, G. Rousse, M. Arroyo y de Dompablo, H. Vezin, J.-M. Tarascon, M. Palacín, *J. Am. Chem. Soc.* **2013**, *135*, 3897 – 3903.
[20] S. Li, Y. Dong, L. Xu, X. Xu, L. He, L. Mai, *Adv. Mater.* **2014**, *26*, 3545 – 3553.

Received: June 8, 2015
Published online: August 18, 2015

